The Interplay Between Developmental Stage and Environment Underlies the Adaptive Effect of a Natural Transposable Element Insertion

Miriam Merenciano and Josefa González*

Institute of Evolutionary Biology (CSIC-Universitat Pompeu Fabra), Barcelona, Spain

***Corresponding author:** E-mail: josefa.gonzalez@csic.es.

Associate editor: Dr. Harmit Malik

Abstract

Establishing causal links between adaptive mutations and ecologically relevant phenotypes is key to understanding the process of adaptation, which is a central goal in evolutionary biology with applications for conservation, medicine, and agriculture. Yet despite recent progress, the number of identified causal adaptive mutations remains limited. Linking genetic variation to fitness-related effects is complicated by gene-by-gene and gene-by-environment interactions, among other processes. Transposable elements, which are often ignored in the quest for the genetic basis of adaptive evolution, are a genome-wide source of regulatory elements across organisms that can potentially result in adaptive phenotypes. In this work, we combine gene expression, *in vivo* reporter assays, CRISPR/Cas9 genome editing, and survival experiments to characterize in detail the molecular and phenotypic consequences of a natural *Drosophila melanogaster* transposable element insertion: the *roo* solo-LTR *FBti0019985*. This transposable element provides an alternative promoter to the transcription factor *Lime*, involved in cold- and immune-stress responses. We found that the effect of *FBti0019985* on *Lime* expression depends on the interplay between the developmental stage and environmental condition. We further establish a causal link between the presence of *FBti0019985* and increased survival to cold- and immune-stress. Our results exemplify how several developmental stages and environmental conditions need to be considered to characterize the molecular and functional effects of a genetic variant, and add to the growing body of evidence that transposable elements can induce complex mutations with ecologically relevant effects.

Key words: **cold-stress, immune-stress, drosophila, transposable elements.**

Introduction

Establishing causal links between mutations and their relevant fitness-related phenotypes is crucial in biology, with implications for evolution, development, and disease (Otwinowski and Nemenman 2013; Mackay and Huang 2018; Nelson et al. 2019). However, causal genotype-phenotype links are difficult to establish since the effect of a mutation can depend on the genetic background (epistasis) as well as on other contexts such as the environment and the developmental stage (Reddy et al. 2009; Kammenga 2017; Young et al. 2019). Because context dependance contributes to diverse traits in diverse organisms, a shift from identifying the impact of a mutation in a particular context to pinpointing the spectrum of effects of a mutation is needed to provide a more realistic picture of the genotype-phenotype map (Eguchi et al. 2019).

Identifying adaptive mutations and analyzing how context dependance influences their effects is even more relevant in the current scenario of rapid environmental change (Catullo et al. 2019; Nelson et al. 2019). To date, most studies that aim at characterizing adaptive mutations have focused on single-nucleotide polymorphism (SNP) variants that are easier to detect by the commonly used short-read sequencing techniques. However, other types of mutations such as transposable elements (TEs), which are known to be a source of adaptive mutations across organisms, have been understudied so far (Hoban et al. 2016). The increased availability of whole genome sequences and advances in sequencing technologies, such as the improvements in long-read sequencing techniques, are fostering the discovery of candidate adaptive TEs (*e.g.* Rech et al. 2022). Besides identifying adaptive mutations at the DNA level, and their fitness-related trait in a relevant ecological context, pinpointing the molecular mechanism by which the mutation influences the phenotype is key to conclude that a mutation has an adaptive effect. TEs can affect gene structure and expression through many different molecular mechanisms (Casacuberta and González 2013; Chuong et al. 2017), and some of these changes have been associated with adaptive phenotypes (Chuong et al. 2016; Ding et al. 2016; Van't Hof et al. 2016; Huang et al. 2018; Esnault et al. 2019; Ullastres et al. 2021; Brosh et al. 2022; Green et al. 2022). In Drosophila, a dual role as enhancer and promoter of an

Article

Open Access

adaptive insertion conferring tolerance to bacterial infection has been recently reported (Ullastres et al. 2021). There are also several examples of TE-induced mutations affecting more than one phenotype, such as the disruption of the *Chkov1* gene leading to resistance to pesticides and to viral infection (Aminetzach et al. 2005; Magwire et al. 2011). Indeed, *D. melanogaster* is an unrivaled model organism to investigate genotype-phenotype links because it has one of the best functionally annotated genomes and powerful tools to genetically modify the organism *in vivo*, which allows not only to identify the molecular mechanism behind the adaptive effect of a mutation but also to demonstrate its causality (Anholt and Mackay 2018).

The *roo* solo-LTR element known as *FBti0019985*, has been previously identified as a candidate adaptive TE insertion: the patterns of nucleotide diversity in its flanking regions suggest that this insertion has increased in frequency due to positive selection (González et al. 2008; Merenciano et al. 2016). *FBti0019985* is inserted in the promoter region of the *Lime* gene, which is located in the first intron of the *cbx* gene (fig. 1). *Lime* is a C_2H_2-type zinc finger transcription factor associated with chill-coma resistance and immune response (Telonis-Scott et al. 2009; Mihajlovic et al. 2019), and *cbx* is a ubiquitin-conjugating enzyme that has also been associated with immune-stress (Ayres et al. 2008; Ullastres et al. 2021). There is previous partial evidence for the association of *FBti0019985* with changes in the expression of its nearby genes, for the molecular mechanisms that might underlie these expression changes, and for *FBti0019985* potential phenotypic effects. Briefly, *FBti0019985* is associated with changes in the expression of its two nearby genes: up-regulation of *Lime* in embryos under nonstress conditions, and down-regulation of *cbx* in adults in nonstress and immune-stress conditions (Merenciano et al. 2016; Ullastres et al. 2021). However, these results were based on the analysis of a limited number of genetic backgrounds, and whether *FBti0019985* is indeed the causal mutation, and if that is the case, whether it also affects *Lime* expression under stress conditions, are still open questions.

The molecular mechanisms underpinning *FBti0019985* effects on gene expression are also not clear yet. There is recent evidence for *FBti0019985* inducing a depletion of the H3K9me3 repressive histone mark in its flanking regions in nonstress conditions (Ullastres et al. 2021). Moreover, while there is evidence for *FBti0019985* providing an alternative transcription start site (TSS) to *Lime* in nonstress conditions (Batut et al. 2013; Merenciano et al. 2016), whether this new transcript is also present in stress conditions and whether it significantly contributes to the increased expression of *Lime* is unknown. Similarly, while *FBti0019985* has been reported to act as an enhancer in response to immune-stress in adults (Villanueva-Cañas et al. 2019), whether the TE also acts as an enhancer in other environmental conditions is also unknown. Finally, previous evidence for the role of *FBti0019985* in egg-to-adult viability is based on association analysis (Merenciano et al. 2016), thus whether *FBti0019985* is the causal mutation and whether it also affects immune-stress survival remain open questions.

In this work, we characterized in detail the molecular and phenotypic effects of *FBti0019985* under cold- and immune-stress conditions, both of them relevant to the survival of *D. melanogaster* in natural environments. We integrated gene expression analysis, *in vivo* reporter assays, *in vivo* Clustered Regularly Interspaced Short Palindromic Repeats (CRISPR/Cas9) genome editing in outbred strains, and survival experiments, to establish a causal link between the presence of the insertion and its ecologically relevant phenotypic effects.

Results

Lime Expression Changes Affect Immune- and Cold-stress Survival and *cbx* Expression Changes Affect Immune-stress Survival

To provide further evidence for the role of *Lime* in cold- and immune-stress and for the role of *cbx* in immune-stress, we performed survival experiments in these two stress conditions using available mutant strains (see Material and Methods). Previous evidence for the role of *Lime* in immune-stress was obtained in larvae after wasp infection, where *Lime* mutants failed to induce systemic metabolic changes needed to develop the immune response (Mihajlovic et al. 2019). To test whether changes in *Lime* expression are also associated with differences in survival to bacterial infection in adult flies, we exposed *Lime* mutant flies to *P. entomophila*. *P. entomophila* is a gram-negative bacterium that orally infects and kills Drosophila in the wild (Vodovar et al. 2005). Using quantitative reverse transcription polymerase chain reaction (qRT-PCR), we first confirmed that $Lime^{MI02952}$ mutant, which contains a MiMIC insertion in the first coding exon of *Lime* (fig. 1), down-regulates *Lime* expression (fig. 2A, supplementary tables S1A and S1B, Supplementary Material online). Because mutations in this genomic region have previously been reported to

Fig. 1. Schematic representation of the genomic region where *FBti0019985* is inserted. *Lime* gene is located in the first intron of *cbx* gene. Light boxes represent untranslated regions (UTRs) and darker boxes represent coding exons. *FBti0019985* insertion overlaps with *Lime* gene. Transcription start sites, including the one that *FBti0019985* adds, are represented as arrows. Transgenic insertion sites are represented with triangles.

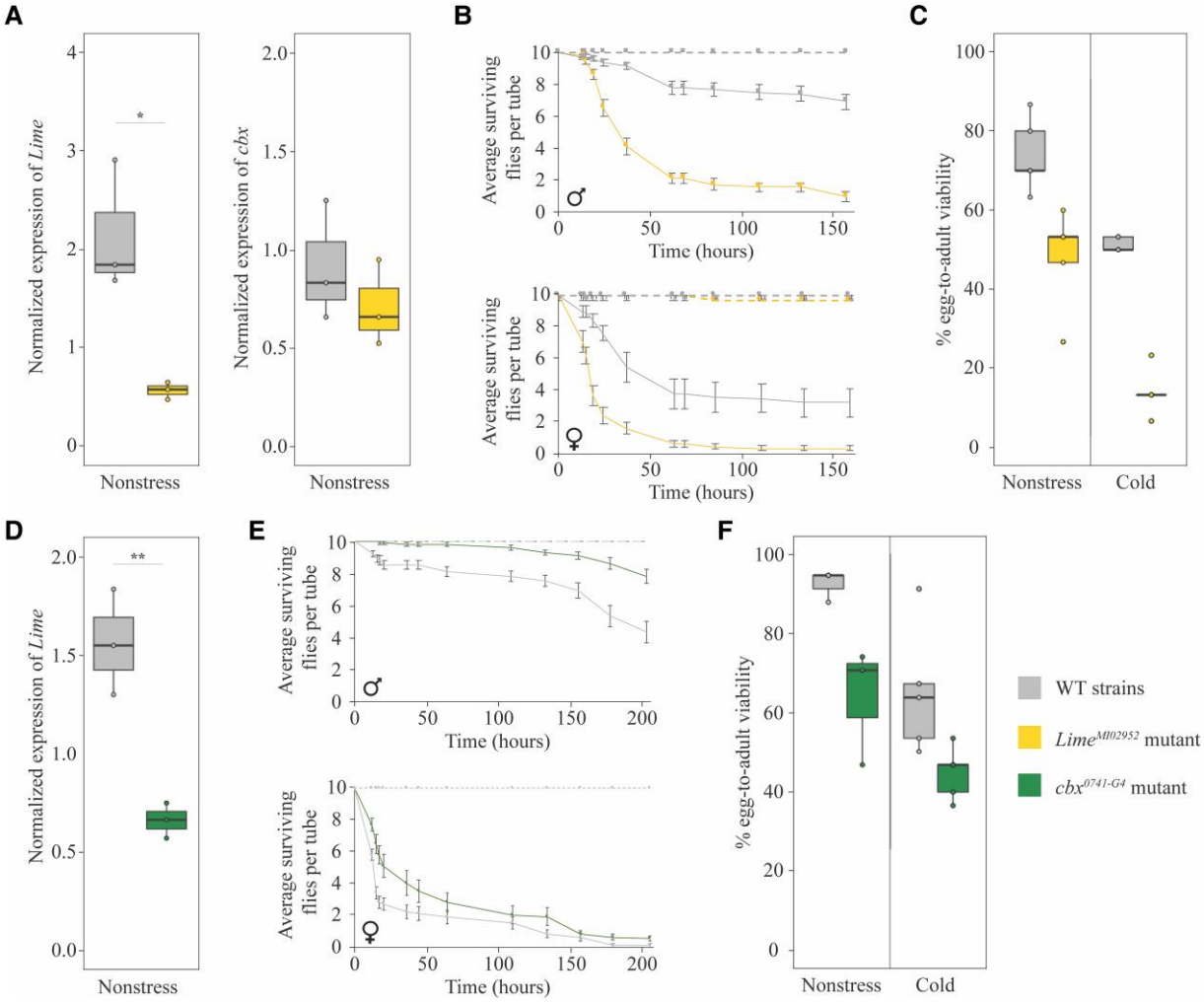

Fig. 2. *Lime* expression changes affect immune- and cold-stress survival and *cbx* expression changes affect immune-stress survival. (*A*) Normalized expression of *Lime* and *cbx* with *Act5C* in the whole-body of $Lime^{MI02952}$ mutant females compared with wild-type (WT) females, which have the same genetic background (supplementary table S1A, Supplementary Material online). Boxplots show the median (horizontal line), first and third quartiles (lower and upper bounds, respectively), and minimum and maximum values (lower and upper whiskers, respectively). For each strain, each dot represents an independent biological replication of a pool of 25 female flies. One-tailed *t*-test *P*-value = 0.015 and 0.400, for *Lime* and *cbx* genes, respectively. (*B*) Survival curves of adult $Lime^{MI02952}$ mutant males and females compared with the WT strain. Survival curves in non-infected conditions are depicted as dotted lines while survival curves after *P. entomophila* infection are depicted as continuous lines. For each strain and sex, each dot represents the average number of surviving flies per tube, for ten replicates of ten flies each (infected conditions), and for three replicates of ten flies each (noninfected conditions). Error bars represent SEM. No mortality was observed in nonstress conditions. Log-rank test was performed to analyze differences between survival curves in infected conditions (log-rank *P*-values < 0.05 both in males and females). (*C*) Egg-to-adult viability in nonstress and cold-stress conditions of $Lime^{MI02952}$ mutants compared with the WT strain. For each strain, each dot represents an independent biological replication of a pool of 30 embryos. Two-way ANOVA: genotype (G: WT/mutant) *P*-value <0.001; experimental condition (EC: nonstress vs. cold-stress) *P*-value <0.001; genotype by experimental condition interaction (GxEC) *P*-value = 0.105. (*D*) Normalized expression of *Lime* with *Act5C* in the whole-body of $cbx^{0741\text{-}G4}$ mutant females compared with WT females. For each strain, each dot represents an independent biological replication of a pool of 25 female flies. One-tailed *t*-test *P*-value = 0.005. (*E*) Survival curves of adult $cbx^{0741\text{-}G4}$ mutant males and females compared with the WT strain. Survival curves in noninfected conditions are depicted as dotted lines while survival curves after *P. entomophila* infection are depicted as continuous lines. For each strain and sex, each dot represents the average number of survival flies per tube, for ten replicates of ten flies each (infected conditions), and for three replicates of ten flies each (noninfected conditions). Error bars represent SEM. No mortality was observed in nonstress conditions. Log-rank test was performed to analyze differences between survival curves in infected conditions (log-rank *P*-value < 0.001 and *P*-value = 0.002 for males and females, respectively. (*F*) Egg-to-adult viability in nonstress and cold-stress conditions of $cbx^{0741\text{-}G4}$ mutants compared with the WT strain. For each strain, each dot represents an independent biological replication of a pool of 30 embryos. Two-way ANOVA: G *P*-value = 0.002; EC *P*-value = 0.003; GxEC *P*-value = 0.528.

affect the expression of both genes (Merenciano et al. 2016; Ullastres et al. 2021), we also tested whether $Lime^{MI02952}$ mutant affects the expression of *cbx*, but found that this was not the case (fig. 2*A*, supplementary table S1B, Supplementary Material online). We then performed survival experiments, and consistent with the previous evidence for the role of *Lime* in immune response (Mihajlovic et al. 2019), we found that *Lime* mutant flies, both male

and females, were more sensitive to *P. entomophila* infection compared with wild-type (WT) flies (Log-rank test *P*-values < 0.001) (fig. 2*B*, supplementary table S1*C*, Supplementary Material online).

Previous works also showed that *Lime* is up-regulated in strains selected for cold-tolerance, and that up-regulation of *Lime* in embryos is associated with increased egg-to-adult viability in nonstress and cold-stress conditions (Telonis-Scott et al. 2009; Merenciano et al. 2016). Consistent with these results, we found that $Lime^{MI02952}$ mutant flies, in which *Lime* expression is down-regulated, showed reduced egg-to-adult viability in nonstress and in cold-stress conditions (fig. 2*C*, supplementary table S1*D*, Supplementary Material online).

Evidence for a role of *cbx* in immune response is based on the analysis of two mutant stocks: cbx^{c00428} and $cbx^{0741\text{-}G4}$, that have a PiggyBac insertion in the first and third intron of *cbx*, respectively (fig. 1). However, although Ayres et al. (2008) found that cbx^{c00428} mutant flies were associated with increased sensitivity to the gram-positive bacteria *S. aureus*, we found that this mutant does not affect *cbx* expression (supplementary table S1*B*, Supplementary Material online) (Ullastres et al. 2021). On the other hand, we found that $cbx^{0741\text{-}G4}$, a null mutant for *cbx* (Ullastres et al. 2021), also down-regulates *Lime* expression (fig. 2*D*, supplementary table S1*B*, Supplementary Material online). Moreover, we confirmed that $cbx^{0741\text{-}G4}$ is associated with increased tolerance to *P. entomophila* infection, as previously suggested by Ullastres et al. (2021) (Log-rank test *P*-value > 0.001 and 0.002 for males and females, respectively) (fig. 2*E*, supplementary table S1*C*, Supplementary Material online). These results suggest that *cbx* indeed plays a role in immune response as *Lime* down-regulation alone is associated with increased sensitivity to *P. entomophila* infection (fig. 2*B*, supplementary table S1*C*, Supplementary Material online), while *Lime* down-regulation and knockout of *cbx* expression in the same genetic background was associated with increased tolerance to infection (fig. 2*E*, supplementary table S1*C*, Supplementary Material online).

Since we found that $cbx^{0741\text{-}G4}$ mutant also down-regulates *Lime* expression, we also checked whether this mutant affects egg-to-adult viability in nonstress and cold-stress conditions, as we have shown that down-regulation of *Lime* is associated with decreased egg-to-adult viability in nonstress and cold-stress conditions (fig. 2*C*). Indeed, we found that $cbx^{0741\text{-}G4}$ mutant showed reduced egg-to-adult viability in nonstress and cold-stress conditions (fig. 2*F*, supplementary table S1*D*, Supplementary Material online).

Overall, our results provide further evidence suggesting that changes in *Lime* expression affect cold- and immune-stress responses and changes in *cbx* expression affect immune-stress response (Ayres et al. 2008; Telonis-Scott et al. 2009; Mihajlovic et al. 2019; Ullastres et al. 2021).

FBti0019985 is Not Associated With Changes of Expression of *cbx* in Response to Immune-Stress

To test whether *FBti0019985* is associated with changes of expression of *cbx* in response to immune-stress, we used two outbred populations: one homozygous for the presence and one homozygous for the absence of the *FBti0019985* insertion in a heterogenous unlinked background (Behrman et al. 2018; Merenciano et al. 2019). Note that previous evidence for an association between *FBti0019985* and *cbx* expression was based on allele specific expression analysis performed in adult guts of the offspring of crosses between an inbred strain homozygous for the presence of the insertion and an inbred strain homozygous for its absence, and concluded that the effect of the insertion was background dependent (Ullastres et al. 2021). We thus performed a qRT-PCR to compare the total expression of *cbx* in adult guts from the outbred populations with and without *FBti0019985* that were orally infected with *P. entomophila*. Note that the gut epithelium is the first barrier that bacteria encounter in the organism and it is known that *P. entomophila* induces strong perturbations in this tissue (Vodovar et al. 2005). We found that, in outbred populations, *cbx* expression was not significantly affected by the insertion genotype (G: presence/absence of *FBti0019985*), the experimental condition (EC: nonstress *vs.* immune-stress), or the interaction between the genotype and the experimental condition (GxEC) (Analysis of variance (ANOVA) *P*-values > 0.05; fig. 3*A* and supplementary table S2, Supplementary Material online), suggesting that the TE does not affect *cbx* expression. We thus focused on the effect of *FBti0019985* on *Lime* for the rest of this work.

FBti0019985 is the Causal Mutation Inducing *Lime* Up-Regulation in Adult Flies Under Immune-Stress

To test for an association between *FBti0019985* and *Lime* expression in nonstress and immune-stress conditions, we used the same two outbred populations described above. We quantified *Lime* expression in adult guts of these two populations as there is previous evidence showing that *FBti0019985* acts as an enhancer in adults in response to immune-stress (Villanueva-Cañas et al. 2019). While no differences in *Lime* expression levels between outbred flies with and without the insertion were found in nonstress conditions, the outbred population with *FBti0019985* had increased *Lime* expression under immune-stress conditions, both in male and female guts (fig. 3*B*, and supplementary table S2, Supplementary Material online). To confirm that the *FBti0019985* is the mutation causing increased *Lime* expression, we generated a precise deletion of the insertion in the outbred population using the CRISPR/Cas9 technique (see Material and Methods). While no differences in expression levels of *Lime* were found in nonstress conditions, under immune-stress, the CRISPR/Cas9 mutant (in which the insertion was deleted) showed *Lime* down-regulation compared with the outbred strain with *FBti0019985*, as

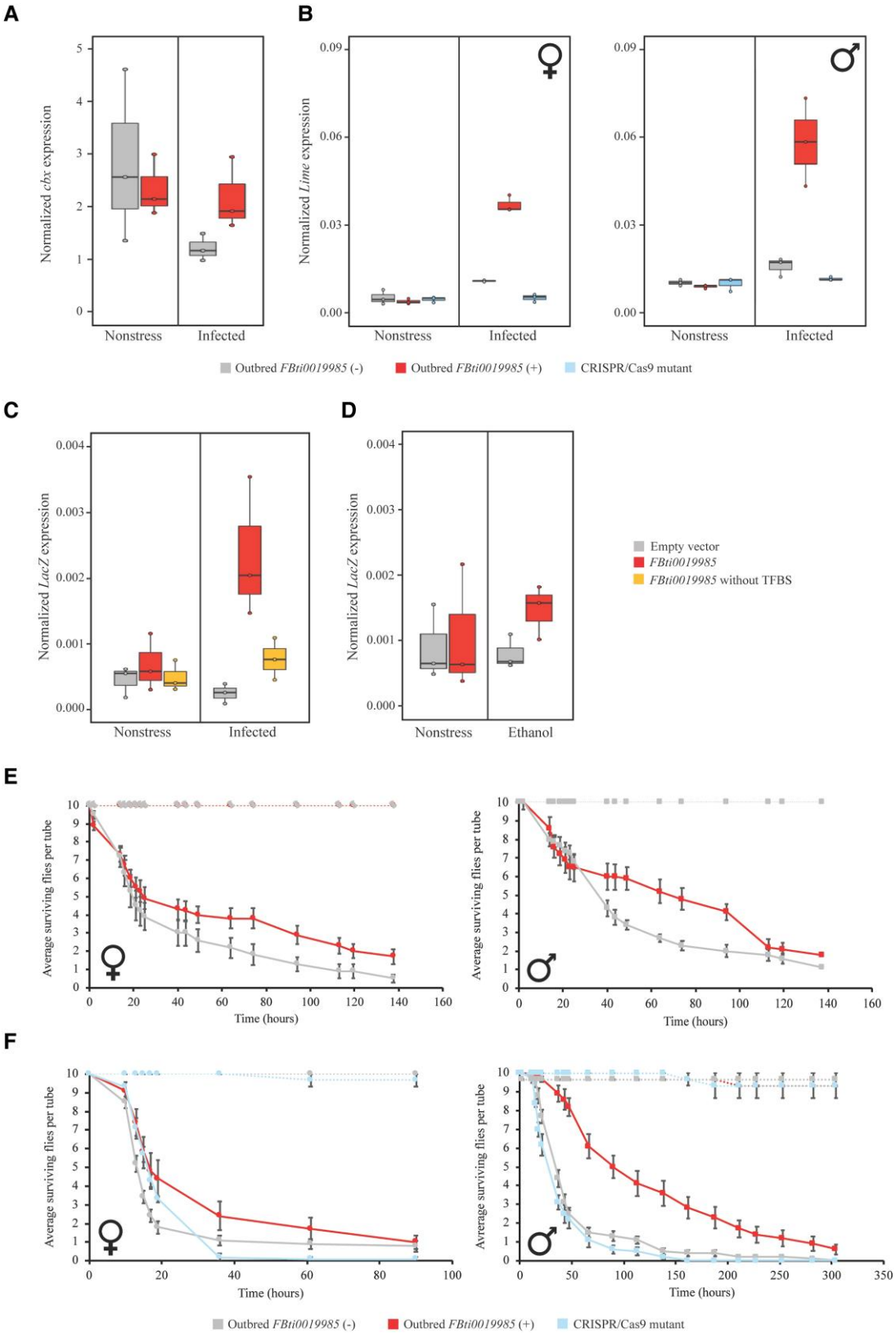

Fig. 3. *FBti0019985* induces *Lime* up-regulation in guts under immune-stress conditions and increases tolerance to *P. entomophila* infection. (*A*) Normalized expression of *cbx* with *Act5C* in adult female guts in nonstress and after *P. entomophila* infection. Boxplots show the median (horizontal line), first and third quartiles (lower and upper bounds, respectively), and minimum and maximum values (lower and upper whiskers, respectively). For each strain, each dot represents an independent biological replicate of a pool of 25–35 guts. Two-way ANOVA: genotype (G: presence/absence of *FBti0019985*) *P*-value = 0.687; experimental condition (EC: nonstress *vs*. immune-stress) *P*-value = 0.138; genotype by

(continued)

expected if this insertion is the causal mutation (fig. 3*B* and supplementary table S2, Supplementary Material online).

Overall, we found that *FBti0019985* was associated with *Lime* up-regulation under immune-stress conditions, and we confirmed using CRISPR/Cas9 to precisely delete the insertion, that *FBti0019985* was the causal mutation (fig. 3*B*).

FBti0019985 Harbors Functional Transcription Factor Binding Sites Related With Immune Response

To identify the molecular mechanism by which *FBti0019985* up-regulates the expression of *Lime* in immune-stress conditions, we first performed *in vivo* enhancer assays. Previous studies have identified several transcription factor binding sites (TFBSs) in the *FBti0019985* sequence (Merenciano et al. 2016; Villanueva-Cañas et al. 2019). Three of these predicted binding sites are for transcription factors *DEAF-1*, *tin*, and *Dorsal*, respectively, which are related to the immune response (Merenciano et al. 2016; Villanueva-Cañas et al. 2019). At least one of these transcription factors, *DEAF-1*, is expressed in the digestive system, which is the first barrier to face oral infections (Larkin et al. 2021). We thus tested whether these immune-related TFBSs could be responsible for *Lime* up-regulation in response to bacterial oral infection, by using directed mutagenesis to delete them from the *FBti0019985* sequence (see Material and Methods), and cloning this modified *FBti0019985* sequence in front of a reporter gene. As expected, we found that the complete sequence of *FBti0019985* drives the expression of the reporter gene in guts in infected conditions (fig. 3*C*, supplementary table S3, Supplementary Material online) (Villanueva-Cañas et al. 2019). When we deleted the three immune-related TFBSs, the expression of the reporter gene was reduced, suggesting that the deleted binding sites were responsible for the enhancer activity of *FBti0019985* in infected conditions (fig. 3*C*, supplementary table S3, Supplementary Material online).

To test whether the enhancer effect of *FBti0019985* is stress-specific, we measured the expression of the reporter gene in adult flies exposed to ethanol-stress. We found no differences in expression under nonstress and ethanol-stress conditions (fig. 3*D*, supplementary table S3, Supplementary Material online). These results confirmed that *FBti0019985* is not acting as an enhancer in nonstress conditions in adult flies, and suggested that the enhancer effect of *FBti0019985* is stress-specific.

Besides acting as an enhancer, *FBti0019985* could also be affecting *Lime* expression by adding a new TSS. TEs of the *roo* family, including *FBti0019985*, have previously been shown to add alternative TSS to nearby genes in embryonic stages (Batut et al. 2013). However, whether the TSS of *FBti0019985* is also used in guts and whether this TSS could contribute to the differential expression of *Lime* in response to immune-stress is unknown. We found that the alternative transcript starting in *FBti0019985* was also present in the gut of adult flies both in nonstress and in immune-stress conditions (supplementary table S2, Supplementary Material online). A transcript-specific qRT-PCR showed that the expression level of the transcript that starts in the TE does not increase significantly under infected conditions (one-tailed *t*-test P-value = 0.352). Moreover, if we compared the expression level of the transcript that starts in the TE with the total *Lime* expression, we found that its contribution, both in nonstress and immune-stress conditions, is low: <1% and 4%, respectively (supplementary table S2, Supplementary Material online).

Overall, we demonstrated that *FBti0019985* harbors functional TFBSs related to immune response that is responsible for its enhancer activity in infected conditions and that this enhancer activity is stress-specific. Although *FBti0019985* is adding a TSS in the gut, the transcript that starts in the TE does not significantly contribute to the increased expression of *Lime* in infected conditions.

Fig. 3. (Continued)
experimental condition interaction (GxEC) P-value = 0.219. (*B*) Normalized expression of *Lime* with *Act5C* in nonstress and immune-stress conditions of adult female and male guts from outbred populations with and without *FBti0019985*, and for CRISPR/Cas9-mutant flies. For each strain, each dot represents an independent biological replicate of a pool of 25–35 guts. Two-way ANOVA outbred *FBti0019985* (+) and outbred *FBti0019985* (−) females: G P-value < 0.001, EC P-value < 0.001, GxEC P-value < 0.001. Two-way ANOVA outbred *FBti0019985* (+) and CRISPR/Cas9 mutant females: G P-value < 0.001, EC P-value < 0.001, GxEC P-value < 0.001. Two-way ANOVA outbred *FBti0019985* (+) and outbred *FBti0019985* (−) males: G P-value = 0.002, EC P-value < 0.001, and GxEC P-value = 0.001. Two-way ANOVA outbred *FBti0019985* (+) and CRISPR/Cas9 mutant males: G P-value = 0.001, EC P-value < 0.001, and GxEC P-value = 0.001. (*C*) Normalized expression of the reporter gene *lacZ* with *Act5C* in adult female guts under nonstress and immune-stress conditions from transgenic flies. Each dot represents an independent biological replicate of a pool of 25–35 guts. Two-way ANOVA empty vector and *FBti0019985* complete sequence: G P-value = 0.009, EC P-value = 0.065, and GxEC P-value = 0.026. Two-way ANOVA *FBti0019985* complete sequence and *FBti0019985* without TFBSs: G P-value = 0.036, EC P-value < 0.024, and GxEC P-value = 0.084. (*D*) Normalized expression of the reporter gene *lacZ* with *Act5C* in transgenic adult female whole-body under nonstress conditions and after ethanol exposure. Each dot represents and independent biological replication of a pool of 25 flies. Two-way ANOVA: G P-value = 0.272, EC P-value = 0.669, and GxEC P-value = 0.494. (*E*) Survival curves of adult outbred female and male flies with and without *FBti0019985* and (*F*) survival curves of adult outbred female and male flies with and without *FBti0019985* and CRISPR/Cas9-mutant flies after *P. entomophila* infection. Survival curves in noninfected conditions are depicted as dotted lines while survival curves after *P. entomophila* infection are depicted as continuous lines. For each strain and sex, each dot represents the average number of survival flies per tube, for ten replicates of ten flies each (infected conditions), and for three replicates of ten flies each (noninfected conditions). Error bars represent SEM. No mortality was observed in nonstress conditions. Log-rank test was performed to analyze differences between survival curves in infected conditions (log-rank P-values < 0.05).

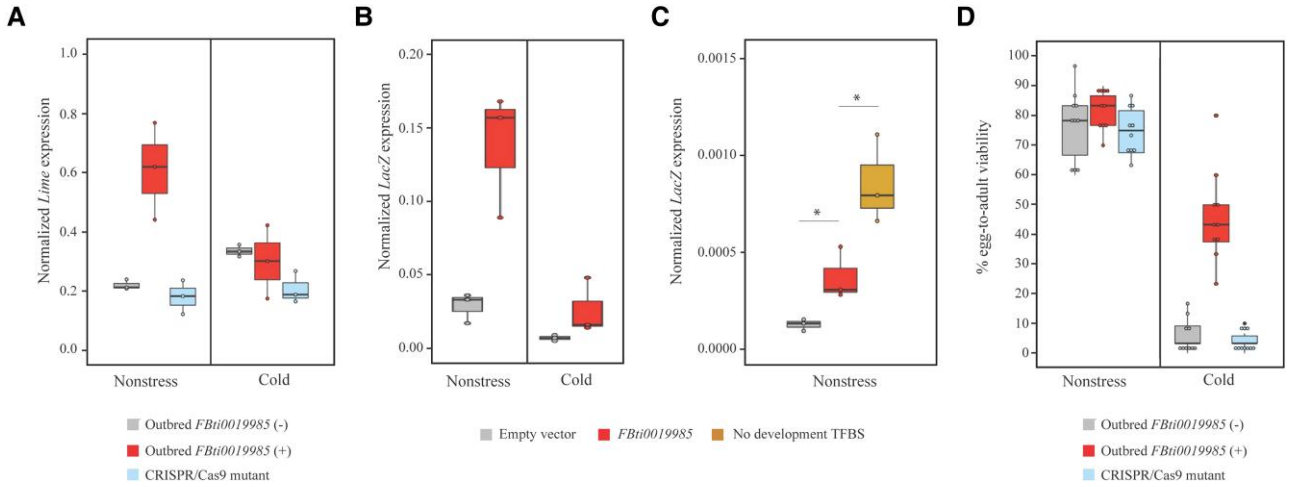

Fig. 4. *FBti0019985* induces *Lime* up-regulation in embryos and increases viability in cold-stress conditions. (*A*) Normalized expression of *Lime* with *Act5C* in nonstress and cold-stress conditions in embryos from outbred populations, and from the CRISPR/Cas9-mutant strain. Boxplots show the median (horizontal line), first and third quartiles (lower and upper bounds, respectively), and minimum and maximum values (lower and upper whiskers, respectively). For each strain, each dot represents an independent biological replication of a pool of approximately 50 embryos. Two-way ANOVA outbred *FBti0019985* (+) and outbred *FBti0019985* (−): genotype (G: presence/absence of *FBti0019985*) *P*-value = 0.018, experimental condition (EC; nonstress *vs.* cold-stress) *P*-value *P* = 0.142, and genotype by experimental condition interaction (GxEC) *P*-value = 0.007. Two-way ANOVA outbred *FBti0019985* (+) and CRISPR/Cas9 mutant: G *P*-value = 0.003, EC *P*-value = 0.056, and GxEC *P*-value = 0.029. (*B*) Normalized expression of the reporter gene *lacZ* with *Act5C* in embryos under nonstress and cold-stress conditions from transgenic flies. For each strain, each dot represents an independent biological replication of a pool of approximately 50 embryos. Two-way ANOVA: G *P*-value = 0.002, EC *P*-value = 0.001, and GxEC *P*-value = 0.012. (*C*) Normalized expression of the reporter gene *lacZ* with *Act5C* in embryos under nonstress conditions from transgenic flies. For each strain, each dot represents an independent biological replication of a pool of approximately 50 embryos. Two-sided *t*-test *P*-values = 0.038 and 0.035 for comparisons between transgenic embryos with the *FBti0019985* complete sequence and transgenic embryos without the TE sequence or *FBti0019985* without development-related TFBSs, respectively. (*D*) Egg-to-adult viability in nonstress and in cold-stress conditions of outbred populations and CRISPR/Cas9 mutant. For each strain, each dot represents an independent biological replication of a pool of 30 embryos. Two-way ANOVA outbred *FBti0019985* (+) and outbred *FBti0019985* (−): G *P*-value < 0.001, EC *P*-value < 0.001, and GxEC *P*-value < 0.001. Two-way ANOVA outbred *FBti0019985* (+) and CRISPR/Cas9 mutant: G *P*-value < 0.001, EC *P*-value < 0.001, and GxEC *P*-value < 0.001.

FBti0019985 Increases Tolerance to *P. entomophila* Infection

To test whether the up-regulation of *Lime* in outbred flies with *FBti0019985* under immune-stress conditions affects fly survival, we performed infection tolerance assays with *P. entomophila*. We found that both female and male flies from outbred populations with *FBti0019985* were more tolerant to infection than flies without the insertion (Log-rank test *P*-value = 0.010 and 0.026, respectively) (fig. 3*E*, supplementary table S4, Supplementary Material online). We repeated the infection tolerance assay including this time the CRISPR/Cas9-mutant strain, which has a precise deletion of the *FBti0019985* insertion. As before, we observed that outbred flies with *FBti0019985* were more tolerant to infection compared with outbred flies without the insertion in both females and males (Log-rank test *P*-value = 0.002 and >0.001, respectively) (fig. 3*F*, supplementary table S4, Supplementary Material online). And, as expected if *FBti0019985* was the causal mutation, the CRISPR/Cas9-mutant strain was more sensitive to infection compared to flies with *FBti0019985* both in females and males (Log-rank test *P*-value = 0.004 and >0.001, respectively) (fig. 3*F*, supplementary table S4, Supplementary Material online).

FBti0019985 Drives *Lime* Up-Regulation in Embryos Under Nonstress Conditions

There is previous evidence associating the presence of *FBti0019985* insertion with increased expression of *Lime* in nonstress conditions in embryos (Merenciano et al. 2016). However, this association was found to be background dependent, and whether *FBti0019985* also affects *Lime* expression in cold-stress conditions has not been tested before (Merenciano et al. 2016). Thus, we checked whether *FBti0019985* affects *Lime* expression in embryos in nonstress and cold-stress conditions. We confirmed that embryos from the outbred population with *FBti0019985* showed *Lime* up-regulation in nonstress conditions compared to embryos from the outbred population without the insertion (fig. 4*A*, supplementary table S2, Supplementary Material online). However, we found no differences in *Lime* expression in cold-stress conditions associated with the presence of the TE (fig. 4*A*, supplementary table S2, Supplementary Material online), further suggesting that the effect of the TE is stress-specific. As expected if *FBti0019985* is the causal mutation, CRISPR/Cas9-mutant embryos showed reduced expression levels of *Lime* in nonstress conditions (fig. 4*A*, supplementary table S2, Supplementary Material online).

Lime Up-Regulation in Embryos is Likely Not Due to Functional Binding Sites in *FBti0019985* Sequence

Consistent with the effect of *FBti0019985* on *Lime* expression in outbred populations, we found that transgenic embryos containing the *FBti0019985* sequence showed significantly increased reporter gene expression only in nonstress conditions (fig. 4*B*, supplementary table S3, Supplementary Material online). *In-silico* predictions found TFBSs related to developmental processes in the *FBti0019985* sequence that could be responsible for this enhancer activity of the TE in embryos (Merenciano et al. 2016). We thus performed an *in vivo* reporter assay deleting the seven development-related predicted binding sites from the TE sequence (*Dorsal*, *Nub*, *ara/mirr* (x2), *Bap*, *Vnd*, and *Btd*) (see Material and Methods). Contrary to our expectations, we did not find reduced expression of the reporter gene when the binding sites were removed from the *FBti0019985* sequence (fig. 4*C*, supplementary table S3, Supplementary Material online). Indeed, we found an increased expression of the reporter gene suggesting that these binding sites might be functional but they were repressing the expression of the reporter gene (fig. 4C, supplementary table S3, Supplementary Material online).

Finally, the level of expression of the transcript that starts in the *FBti0019985* insertion was not significantly different in nonstress and cold-stress conditions (one-tailed *t*-test *P*-value = 0.174). In embryos, the contribution to the total *Lime* expression of the transcript that starts in the TE was higher than the one observed in adults (13.6% and 10.2% in nonstress and stress, respectively *vs*. <1% and 4%; supplementary table S2, Supplementary Material online), as expected since *roo* elements are known to provide embryonic promoters (Batut et al. 2013).

FBti0019985 Increases Egg-to-Adult Viability Under Cold-Stress Conditions

We checked the egg-to-adult viability of outbred strains with and without *FBti0019985* in nonstress and in cold-stress conditions. We found that the insertion genotype (presence/absence of *FBti0019985*), the experimental condition (nonstress *vs*. cold-stress), and the interaction between the genotype and the experimental condition were significant (fig. 4*D*, supplementary table S5, Supplementary Material online). As expected if *FBti0019985* is the causal mutation, CRISPR/Cas9-mutants showed reduced viability compared with the outbred strain with the element in cold-stress conditions (fig. 4*D*, supplementary table S5, Supplementary Material online).

roo Insertions Are Not Enriched Nearby Immune-Stress Genes

Our results show that the *FBti0019985 roo* insertion increases the expression of *Lime* in response to immune-stress by adding functional immune-related TFBS, leading to increased survival to bacterial infection (fig. 3). We thus checked whether other *roo* insertions in the genome were enriched nearby immune-stress response genes. We focused on the 157 *roo* insertions present in the last release of the *D. melanogaster* reference genome (r.6.48) and identified those that are inserted nearby (<1 kb) candidate genes involved in immune-stress (see Material and Methods). Overall, we found that 10 of the 157 *roo* insertions were inserted nearby immune-related genes (supplementary table S7, Supplementary Material online). However, there was no significant enrichment of *roo* insertions nearby immune-related genes (one-side Fisher's exact test $P = 0.094$) (supplementary table S7, Supplementary Material online).

Discussion

In this work, we characterized a naturally occurring TE-induced mutation and found that the effect of the mutation depends on the interplay between the environmental condition and the developmental stage (fig. 5). While in nonstress conditions the *FBti0019985* insertion only affects *Lime* expression in embryos, in stress conditions *FBti0019985* affects *Lime* expression in adults, and specifically in response to immune-stress (figs. 3–5). CRISPR/Cas9-mediated deletion of the insertion in an outbred population confirmed that the TE is the causal mutation leading to *Lime* up-regulation in nonstress in embryos and immune-stress in adults. Furthermore, we showed that *FBti0019985* is the causal mutation leading to increased bacterial infection tolerance and increased viability in cold-stress conditions (figs. 3–5). Previous evidence for the complex effects of TE-induced mutations was mostly associated with coding mutations (Wang et al. 2018; Frank et al. 2022). For instance, *Syncytin-1*, a human-endogenous retrovirus gene with a clear role in human placental formation (Mi et al. 2000; Senft and Macfarlan 2021), has also been associated with the development of neuropsychological disorders and multiple sclerosis under certain environmental stress conditions such as infection, or drug application (Gröger and Cynis 2018; Wang et al. 2018). Similarly, *Supressyn*, another gene from a retroviral origin also involved in placental development, has been recently linked with resistance to viral infection, demonstrating that its effect is context-dependent (Frank et al. 2022). Our results thus showed that besides TE-induced coding mutations, the effect of TE-induced regulatory mutations is also complex, further suggesting that TEs could be more likely to have complex effects compared to SNPs (e.g., a single mutation can add both promoters and TFBS) (Schrader and Schmitz 2019; Baduel and Quadrana 2021).

Besides adding an alternative TSS to *Lime*, *FBti0019985* also acts as an enhancer (Batut et al. 2013; Merenciano et al. 2016). There is increasing evidence across organisms that regulatory regions can have a dual function as both promoters and enhancers (Dao and Spicuglia 2018; Andersson and Sandelin 2020). Indeed, in Drosophila, 4.5% of enhancer sequences overlap with TSS (Arnold

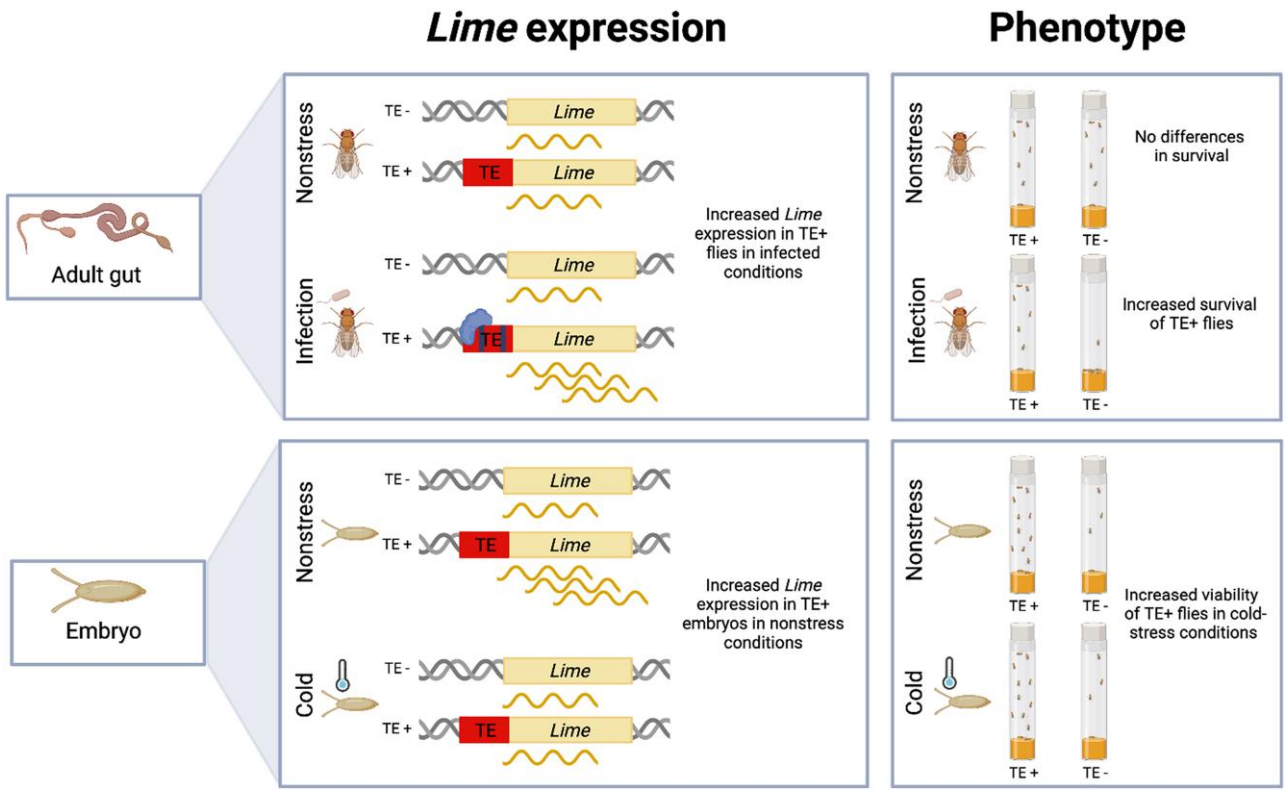

Fig. 5. Schematic representation of the effect of *FBti0019985* in nonstress, infected, and cold-stress conditions. Flies with the *FBti0019985* insertion show increased *Lime* expression in guts in infected conditions due to the presence of functional immune-related TFBSs in the TE sequence. These differences in *Lime* expression are responsible for the increased survival from infection in flies with the insertion. Embryos with *FBti0019985* show an increased *Lime* expression in nonstress conditions, and increased viability in cold-stress conditions. The molecular mechanism of increased expression in embryos in nonstress conditions remains to be uncovered. Big boxes represent *Lime* gene, while small boxes represent the *FBti0019985* TE insertion. Wavy lines represent *Lime* transcripts. Functional TFBSs in the *FBti0019985* sequence are depicted as small rectangles within *FBti0019985*.

et al. 2014; Zabidi et al. 2015). TE insertions have been documented to contribute to gene regulation by functioning as enhancers (Barco et al. 2019; Sundaram and Wysocka 2020) and promoters (Faulkner and Carninci 2009; Batut et al. 2013), and recently a dual role as both enhancer and promoter in immune-stress conditions has been described for *FBti0019386*, a natural TE insertion in *D. melanogaster* (Ullastres et al. 2021). However, unlike *FBti0019386*, the alternative transcript starting in *FBti0019985* does not seem to have a significant contribution to the changes in gene expression in the developmental stages and conditions analyzed in this work. Thus, characterization of other TEs with the potential to increase transcript diversity and to act as enhancers is needed to evaluate the contribution of this type of mutations to complex regulatory regions.

Our results also suggest that the molecular mechanism by which a TE increases the expression of its nearby gene could be different in nonstress versus stress conditions. While we found that the insertion harbors functional binding sites for immune-related transcription factors (fig. 3C), a mechanism other than adding binding sites appears to be responsible for the enhancer role in embryonic stages (fig. 4C). Although we cannot discard that TFBS not identified in this work are responsible for the enhancer activity of *FBti0019985* in embryos, other mechanisms such as inducing epigenetic changes could also be responsible for the observed changes in expression (Rey et al. 2016; Guio et al. 2018; Ullastres et al. 2021).

Finally, we speculate that the effect of *Lime* on sugar metabolism might underlay the increased immune- and cold-stress survival observed (figs. 3 and 4) (Mihajlovic et al. 2019). *Lime* affects the levels of glucose and trehalose, which has been shown to affect immune cell proliferation and activation (Mihajlovic et al. 2019). Moreover, changes in glucose and trehalose have been reported in cold-shock and rapid cold-hardening treatments in *D. melanogaster* (Overgaard et al. 2007; Koštál et al. 2011). Thus, increased basal levels of *Lime* expression in embryos might be beneficial when flies are exposed to cold-stress. Indeed, distinct basal transcriptional states have been associated with different phenotypic responses to enteric infection and also to cold-stress in *D. melanogaster* (Telonis-Scott et al. 2009; Bou Sleiman et al. 2015). However, further experiments are needed to link the effect of *FBti0019985* on *Lime* expression with changes in sugar metabolism and its subsequent effects on cold and immune tolerance.

Overall, this work provides evidence for *FBti0019985* being the causal mutation responsible for *Lime* up-regulation as a result of the interplay between the developmental stage and environment. We further demonstrate that *FBti0019985* increases viability in cold-stress and immune-stress. These results open up the question of how often tissue-specific and environment-dependent gene expression could be due to the presence of TEs and call for their inclusion in studies aimed at understanding the context-dependent effect of mutations. Furthermore, our results provide support for the need to expand the concept of the genotype-phenotype map from identifying the impact of a mutation in a particular context to exploring the spectrum of effects in different contexts, including different genetic backgrounds, environments, and developmental stages.

Materials and Methods

Fly Stocks

Fly stocks were reared on standard fly food medium containing glucose, fresh yeast, wheat flour, agar, propionic acid, and nipagin in a 12:12 h light/dark cycle at 25 °C.

Laboratory Mutant and RNAi Knock-Down Strains

We used three laboratory mutant strains and one RNAi knock-down strain that were likely to affect *Lime* and/or *cbx* genes. We also used two wild-type (WT) strains with the same genetic backgrounds as the mutant strains, and a strain with a GAL4 promoter to activate the RNAi (supplementary table S1A, Supplementary Material online). Briefly, we used $Lime^{MI02952}$ mutants (Bloomington Drosophila Stock Center stock number #36170) that contain a MiMIC insertion in the first exon of *Lime* gene. As a WT strain, we used *y[1] w[67c23]* flies (stock number #6599) with the same genetic background (supplementary table S1A, Supplementary Material online). We used a RNAi knock-down strain for the same gene (stock number #33735) (supplementary table S1A, Supplementary Material online). To activate the RNAi, that strain was crossed to a strain containing a GAL4 promoter (w; act GAL4/TM6 + tb) (supplementary table S1A, Supplementary Material online). We also used $cbx^{0741\text{-}G4}$ mutants (stock number #63767) and cbx^{c00428} mutants (stock number #10067) with a PiggyBac insertion in the first and third intron of *cbx*, respectively. For these two mutants, we used as a WT the strain *w1118*, which has the same genetic background as the two mutant strains (supplementary table S1A, Supplementary Material online).

Outbred Strains

We used the two outbred populations, one with and one without *FBti0019985* TE insertion, generated by Merenciano et al. (2019). Briefly, they were generated by a round-robin cross-design of inbred lines from the Drosophila genetic reference panel (Mackay et al. 2012) and isofemale lines from different European populations (Merenciano et al. 2019). Outbred populations were maintained by random mating with a large population size for over five generations before starting the first experiments.

CRISPR/Cas9 Mutant Strains

To generate a CRISPR/Cas9 strain with a precise deletion of *FBti0019985* in the natural outbred population we followed a two-step approach (Merenciano and González 2023). First, we substituted the insertion by the DsRed fluorescence marker and then, in a second step, we removed the visual marker to avoid any possible effect of the introduced DsRed sequence in the results (supplementary fig. S1, Supplementary Material online). For the substitution of *FBti0019985* by the DsRed fluorescence marker, guide RNAs (gRNA1: 5′-tatctcaaat aagtctagct-3′ and gRNA2: 5′-cagagaaacgtcgagctgcg-3′) were designed in the *FBti0019985* flanking region using the flyCRISPR target finder (http://targetfinder.flycrispr.neuro.brown.edu/). Both gRNAs1 and gRNA2 were cloned into pCFD5 plasmid following the pCFD5 cloning protocol (www.crisprflydesign.com) (Port and Bullock 2016) using the primers 5′-gcggcccgggttcgattcccggccgatgcaagctagactt atttgagatagttttagagctagaaatagcaag-3′ and 5′-attttaactt gctatttctagctctaaaaccagagaaacgtcgagctgcgtgcaccagccgggaa tcgaaccc-3′, that contain gRNA1 and gRNA2 sequences, respectively. Briefly, these primers are used on a pCFD5 template and the resulting PCR products are assembled with a previously linearized pCFD5 backbone (digested with the BbsI type II-S restriction enzyme [NEB]) in a single Gibson Assembly reaction. A donor DNA containing two homology arms flanking the DsRed sequence for homology repair was cloned into the pHD-ScarlessDsRed plasmid (https://flycrispr.org/scarless-gene-editing/) using the Q5® High-Fidelity DNA polymerase kit (New England Biolabs). Left homology arm contained the sequence in 2R:9870299–9871095 (FlyBase Release 6) (Larkin et al. 2021) while the right homology arm contained the sequence in 2R:9871529–9872365 (FlyBase Release 6) (Larkin et al. 2021) from the outbred population with *FBti0019985*. To avoid cleavage of the donor construct and mutagenesis after integration by CRISPR/Cas9, two single-nucleotide synonymous substitutions (C > G for sgRNA1; G > T for sgRNA2) were introduced into the two sgRNA target site protospacer adjacent motif (PAM) sequences, respectively. The pCFD5 plasmid containing the gRNAs, the donor pHD-ScarlessDsRed plasmid containing the homology arms, and a plasmid containing Cas9 endonuclease were co-injected as a unique mix into approximately 550 embryos from the outbred population with *FBti0019985*. All the injections were performed using the following mix concentrations: pCFD5 plasmid at 100 ng/µl, donor plasmid at 500 ng/µl, and Cas9 plasmid at 250 ng/µl. F_0-emerged flies were backcrossed individually with the parental outbred population with *FBti0019985*, and F_1 offspring was screened for eye fluorescence. These flies were backcrossed again individually with the parental line for a minimum of five generations to

remove potential off-targets generated during the process (Bassett and Liu 2014; Port et al. 2020). Then, we performed crosses between flies expressing eye fluorescence, to esta blish an outbred population homozygous for the deletion of *FBti0019985*. The substitution of *FBti0019985* by DsRed was checked by PCR with two combinations of primers in each cross: forward primer 5′-aacaatgcaagtccgtgctc-3′ and reverse primer 5′-gtggttcctccacccttgtg-3′ spanning the whole substituted region; and forward primer 5′-ggccgcga ctctagatcataatc-3′ (inside DsRed sequence) and reverse primer 5′-gtggttcctccacccttgtg-3′ to check for the absence of substitution events. PCR bands were confirmed by Sanger sequencing.

In the second step, to remove the DsRed sequence, we applied again the CRISPR/Cas9 technique designing two gRNAs (gRNA3: 5′-ttgaacactaatgacaattt-3′and gRNA4: 5′-gagctgcgcagttgtgagct-3) in the flanking regions of the DsRed sequence using the flyCRISPR target finder as before. Both gRNA3 and gRNA4 were cloned into the pCFD5 plasmid following the pCFD5 cloning protocol as mentioned above using the primers 5′-gcggcccgggttcg attcccggccgatgcttgaacactaatgacaatttgttttagagctagaaatagca ag-3′ and 5′-attttaacttgctatttctagctctaaaacagctcacaactgc gcagctctgcaccagccgggaatcgaaccc-3′, that contain the gRNA3 and gRNA4 sequences, respectively. A donor DNA containing only two homology arms for homolog y-directed repair was cloned into the pHD-ScarlessDsRed plasmid removing the DsRed sequence. Left homology arm contained the sequence in 2R:9870299–9871095 (FlyBase Release 6) (Larkin et al. 2021) while the right homology arm contained the sequence in 2R:9871529–9872365 (FlyBase Release 6) (Larkin et al. 2021) from the outbred population with *FBti0019985* adding two single-nucleotide synonymous substitutions (G > A for sgRNA3 site; C > T for sgRNA4 site). The pCFD5 plasmid containing the gRNAs 3 and 4, the donor pHD-Scarless plasmid containing the homology arms, and a plasmid containing Cas9 endonuclease were co-injected as explained before into embryos from the previously generated CRISPR/Cas9 mutant containing the DsRed fluorescent marker and the *FBti0019985* deletion. F_0-emerged flies were backcrossed individually with the CRISPR/Cas9 mutant without *FBti0019985*, and F_1 offspring was screened this time for the absence of eye fluorescence. These flies were backcrossed again individually for a minimum of five generations to remove potential off-targets generated during the process. Then, performing crosses between flies not expressing eye fluorescence, an outbred population containing a homozygous deletion of DsRed was established. The DsRed deletion was checked by PCR in each cross using the primer pair 5′-aaca atgcaagtccgtgctc-3′ and 5′-cgtaggatcagtgggtgaaaatg-3′, and finally, PCR bands were confirmed by Sanger sequencing. No polymorphism were found in the sequenced reg ion except for the two single-nucleotide synonymous substitutions introduced into the two sgRNA target site PAM sequences.

Transgenic Strains

For the *in vivo* reporter assays, we used the transgenic flies with the *FBti0019985* sequence cloned in front of the *lacZ* reporter gene generated in Ullastres et al. (2021), and we compared them with transgenic strains with the placZ.attB empty vector to control for possible *lacZ* expression driven by the vector sequence itself. To generate the transgenic flies with deleted TFBSs, we performed directed mutagenesis for each TFBS using the placZ.attB vector containing the *FBti0019985* sequence as a template (Ullastres et al. 2021), with the Q5 site-directed mutagenesis kit (New England Biolabs). Since it is not possible to delete several TFBSs at the same time, we performed consecutive deletions until all the binding sites were deleted. Primers used for deleting each TFBSs can be found in supplementary table S6, Supplementary Material online. Then, the vector with the *FBti0019985* sequence with the immune-related TFBSs deleted (*DEAF-1*, *tin*, and *Dorsal*) and the vector with the developmental TFBSs deleted (*Dorsal*, *Nub*, *ara/mirr* (x2), *Bap*, *Vnd*, and *Btd*) were microinjected separately at 350–500 ng/µl into a *D. melanogaster* strain with a stable docking site in the chromosome 2 (Bloomington Stock number: #24749). Offspring was screened for red eyes and the insertion of the construct was verified by PCR and Sanger sequencing with the primer pair 5′-ggtgggcataatagtgttgtttat-3′ and 5′-cgacgtgtt cactttgcttgt-′3. Three independent homozygous stocks were generated and used as biological replicates for the qRT-PCR experiments.

Sample Collection for Expression Analysis

Laboratory Mutant and RNAi Knock-Down Strains

5–7 day-old females from each strain were harvested and placed in vials with fresh food in groups of 25. We allowed the flies to recover from CO_2 anesthesia for 24 h at 25 °C. Then, the pool of 25 females of every strain was placed in three empty Eppendorf tubes and considered as independent replicates. Finally, samples were flash-frozen in liquid nitrogen and stored at −80 °C until sample processing. *Lime* and *cbx* expression changes were measured in the $Lime^{MI02952}$ mutants compared with a strain with the same genetic background (*y[1] w[67c23]*) (supplementary table S1A and B, Supplementary Material online). We also measured *Lime* and *cbx* expression in the offspring of the cross between the *Lime-RNAi* strain and a strain expressing the GAL4 promoter for the activation of the RNAi (*w; act GAL4/TM6 + tb*). We compared the expression of the offspring with the maternal strain containing the GAL4 promoter (supplementary table S1A and B, Supplementary Material online). *Lime* expression was measured in $cbx^{0741\text{-}G4}$ and cbx^{c00428} mutants, comparing both of them to a strain with the same genetic background (*w1118*) (supplementary table S1A and B, Supplementary Material online). Only $Lime^{MI02952}$ mutants that affected *Lime* expression and $cbx^{0741\text{-}G4}$ mutants that

affected *cbx* and *Lime* expression were used in the phenotypic assays (supplementary table S1B, Supplementary Material online).

P. entomophila Infection in Outbred Populations and CRISPR/Cas9 Mutants

5–7 day-old flies from each strain tested were separated by sex and placed in vials with fresh food in groups of 25–35. We allowed flies to recover from CO_2 anesthesia for 24 h at 25° C. To expose the flies to the gram-negative bacteria *P. entomophila* infection, we followed the protocol described in Neyen et al. (2014). Briefly, after two hours of starvation, we transfer 75–105 flies in groups of 25–35 into three vials with fresh food and a filter paper soaked with 120 µl of a solution containing 1.25% sucrose and bacterial preparation adjusted to a final $OD_{600} = 50$ for females and $OD_{600} = 150$ for males. These bacterial loads were chosen so that the mortality observed after the 12 h of treatment was <70%. Flies were kept at 29 °C, the optimal temperature condition for *P. entomophila* infection. Simultaneously, a total of 75–105 flies were also transferred in groups of 25–35 into three vials with fresh food and a filter paper soaked with 120 ul of a solution containing sterile lysogeny broth (LB) medium with 1.25% sucrose and kept at 29 °C as a control. Guts from males and from females of every one of the three vials were dissected after 12 h and considered as independent replicates. Samples were then flash-frozen in liquid nitrogen and stored at −80 °C until sample processing.

Cold-stress Treatment in Outbred Populations and CRISPR/cas9 Mutants

5–7 day-old flies from each strain tested were allowed to lay eggs at 25 °C in a fly cage with egg-laying medium (2% agar with apple juice and a piece of fresh yeast) for four hours. After these four hours, adults were removed and the plate containing embryos was kept at 1 °C for four additional hours. Simultaneously, another plate with embryos was kept at 25 °C for four additional hours as a control. 4–8 h-old embryos were then collected from both plates using the method described in Schou (2013). Briefly, eggs laid on the surface of the egg-laying medium were gently washed with a sucrose solution (29 g/100 mL sucrose/water) with a small brush and poured into an Erlenmeyer flask with a mesh to keep the embryos. Then, embryos were dechorionated for 10 min with 50% bleach. A pool of approximately 50 dechorionated embryos of every strain and treatment was placed in three different empty eppendorf tubes and considered as independent replicates. Finally, samples were flash-frozen in liquid nitrogen and stored at −80 °C until sample processing.

Ethanol Exposure in Transgenic Strains

5–7 days-old flies from each strain tested were separated by sex and placed in vials with fresh food in groups of 25. We allowed flies to recover from CO_2 anesthesia for 24 h at 25 °C. To expose the flies to ethanol we followed the method described in Maples and Rothenfluh (2011). Briefly, 150 flies in groups of 25 were transferred into six empty vials. A coated cotton ball with 0.5 ml ethanol was inserted into three vials (exposure vials) for nine minutes ensuring that the alcohol was facing into the vial and not toward the wall. Simultaneously, coated cotton balls with 0.5 ml H_2O were inserted into the remaining three vials (control vials). After that, flies of each vial were transferred to empty eppendorf tubes and considered as independent replicates. Finally, samples were flash-frozen in liquid nitrogen and stored at −80 °C until processing.

RNA Extraction and cDNA Synthesis

RNA was extracted using the GeneEluteTM Mammalian Total RNA Miniprep Kit following manufacturer's instructions (Sigma). RNA was then treated with DNase I (Thermo 1 U) for 1 h at 37 °C. cDNA was then synthesized from a total of 250–1,000 ng of RNA using the NZY First-Strand cDNA synthesis kit (NZYTech).

qRT-PCR Analysis

Lime expression was measured using the forward primer 5′ -gagcagttggaatcgggttttac −3′ and the reverse primer 5′-gtatgaatcgcagtccagccata-3′ spanning 99 bp cDNA in the exon 1/exon 2 junction. *cbx* expression was measured with the forward primer 5′-gggaaaacgatctgggagca −3′ and the reverse primer 5′- gtcggagaagttgagtggga −3′ spanning 233 bp cDNA in the exon 2/exon 3 junction. *lacZ* reporter gene expression was measured using the forward primer 5′-cctgctgatgaagcagaacaact-3′ and the reverse primer 5′-gctacggcctgtatgtggtg-3′. Gene expression was normalized with *Act5C* (5′ -gcgcccttactctttcacca-3′ and 5′ -atgtcacggacgatttcacg-3′ primers). We performed the qRT-PCR analysis with SYBR green (BioRad) or with the qPCRBIO SyGreen Mix Lo-Rox (PCRBiosystems) on iQ5 and CFX384 Thermal cyclers, respectively. Results were analyzed using the difference between cycle threshold (dCT) method (Pfaffl 2001).

Transcript Start Site Detection

We performed RT-PCRs to detect whether *FBti0019985* is adding an alternative TSS to the *Lime* gene in outbred flies carrying *FBti0019985* after different stress conditions. We used the forward primer 5′- aaaactcaacgagtaaagtcttc −3′ and the reverse primer 5′- tataaagttccaacgcccagc −3′ to detect the *Lime* transcript starting in the TE. The forward primer 5′- cgcagagaaacgtcgagctg −3′ and the reverse primer 5′-cacgttaaattcactagggtggc −3′ were used to detect *Lime* total transcript. The outbred population without *FBti0019985* was used as a control sample.

Phenotypic Assays

P. entomophila Infection

Ten tubes of ten 5–7 day-old male flies and ten tubes of ten 5–7 day-old females from each one of the strains tested were infected with the gram-negative bacteria *P. entomophila* as described before (total $n = 100$ flies per sex).

Simultaneously, a total of three tubes of ten male and three tubes of ten female flies were tested as controls (total $n = 30$ flies per sex). We counted the number of dead flies in every vial at different time points for at least six days. Log-rank tests (Mantel-Cox) were performed to analyze pairwise differences between survival curves with SPSS v21 software.

Egg-to-Adult Viability Under Cold-Stress

5–7 day-old flies from each strain tested were allowed to lay eggs for 4 h at 25 °C in a fly cage with egg-laying medium (2% agar with apple juice and a piece of fresh yeast) for four hours. Then, adults were removed from the cage and plates were kept for four additional hours at 25 °C. After that, 4–8 h-old embryos were collected using the method described in Schou (2013) and placed in vials with fresh food in groups of 30. Briefly, eggs laid on the surface of the egg-laying medium were gently washed with a sucrose solution (29 g/100 mL sucrose/water) with a small brush and poured into an Erlenmeyer flask with a mesh to keep the embryos. Then, embryos were transferred with a small brush in the surface of a filter paper moistened with the sucrose solution, counted under a magnifying glass, and finally placed into tubes with fresh food. Then, a pool of 30 embryos of every strain was transferred to 20 empty vials with fresh food (ten vials for the experiment with mutant flies) and considered as independent replicates. Ten vials (five for the experiment with mutant flies) were kept at 1 °C for 15 h and then maintained at 25 °C until adult emergence. Simultaneously, ten control vials (five for the experiment with mutant flies) were kept at 25 °C and never exposed to cold. Percentage egg-to-adult viability was calculated based on the number of emerged flies to the total number of embryos placed in each vial. Statistical significance was calculated by performing ANOVA using SPSS v.21 combining all the data into a full model: experimental condition (stress and nonstress), insertion genotype (presence/absence of the insertion), and interaction between these two factors.

roo Enrichment Nearby Immune-Stress Candidate Genes

We used the last available TE annotation of the reference genome (http://ftp.flybase.net/genomes/Drosophila_melanogaster/dmel_r6.48_FB2022_05/fasta/dmel-all-transposon-r6.48.fasta.gz) to build a *bed* file with the coordinates and names of all the 157 *roo* insertions using the commands *egrep* and *awk*. To know how many of these copies were inserted near immune-stress candidate genes (<1 kb), we used previously available information that summarizes evidence from genome-wide association studies (GWAS), quantitative trait loci (QTL), gene expression, and protein–protein interactions, and candidate gene studies to identify genes involved in immune-stress (Rech et al. 2019). We thus generated a file with a list of 971 candidate genes (supplementary table S7A, Supplementary Material online). We then created a *bed* file with the coordinates of these genes using the *gtf* file of the last release of the reference genome (http://ftp.flybase.net/genomes/Drosophila_melanogaster/dmel_r6.48_FB2022_05/gtf/dmel-all-r6.48.gtf.gz) and the commands *egrep* and *awk*. Then, we used *bedtools windows* with default parameters to obtain the *roo* insertions present in <1 kb distance of our candidate immune-stress related genes (supplementary table S7B, Supplementary Material online). Statistical significance was calculated by performing Fisher's exact test.

Supplementary Material

Supplementary data are available at *Molecular Biology and Evolution* online.

Acknowledgments

We thank Fillip Port from the Division of Signaling and Functional Genomic led by Prof. Dr. Michael Boutros for his advice in the generation of the CRISPR/Cas9 mutants. This project has received funding from the European Research Council (ERC) under the European Union's Horizon 2020 research and innovation program (H2020-ERC-2014-CoG-647900).

Author Contributions

M.M. and J.G. designed research; M.M. performed research; M.M. and J.G. analyzed data; and M.M. and J.G. wrote the paper.

Data Availability

The data is available within the Article and Supplementary Information.

Conflict of interest statement: The authors declare no competing interest.

References

Aminetzach YT, Macpherson JM, Petrov DA. 2005. Pesticide resistance via transposition-mediated adaptive gene truncation in Drosophila. *Science* **309**(5735):764–767.

Andersson R, Sandelin A. 2020. Determinants of enhancer and promoter activities of regulatory elements. *Nat Rev Genet*. **21**(2):71–87.

Anholt RRH, Mackay TFC. 2018. The road less traveled: from genotype to phenotype in flies and humans. *Mamm Genome*. **29**(1–2):5–23.

Arnold CD, Gerlach D, Spies D, Matts JA, Sytnikova YA, Pagani M, Lau NC, Stark A. 2014. Quantitative genome-wide enhancer activity maps for five Drosophila species show functional enhancer conservation and turnover during cis-regulatory evolution. *Nat Genet*. **46**(7):685–692.

Ayres JS, Freitag N, Schneider DS. 2008. Identification of Drosophila mutants altering defense of and endurance to Listeria monocytogenes infection. *Genetics* **178**(3):1807–1815.

Baduel P, Quadrana L. 2021. Jumpstarting evolution: how transposition can facilitate adaptation to rapid environmental changes. *Curr Opin Plant Biol*. **61**:102043.

Barco B, Kim Y, Clay NK. 2019. Expansion of a core regulon by transposable elements promotes Arabidopsis chemical diversity and pathogen defense. *Nat Commun*. **10**(1):3444.

Bassett A, Liu JL. 2014. CRISPR/Cas9 mediated genome engineering in Drosophila. *Methods* **69**(2):128–136.
Batut P, Dobin A, Plessy C, Carninci P, Gingeras TR. 2013. High-fidelity promoter profiling reveals widespread alternative promoter usage and transposon-driven developmental gene expression. *Genome Res*. **23**(1):169–180.
Behrman EL, Howick VM, Kapun M, Staubach F, Bergland AO, Petrov DA, Lazzaro BP, Schmidt PS. 2018. Rapid seasonal evolution in innate immunity of wild. *Proc Biol Sci*. **285**(1870):20172599.
Bou Sleiman MS, Osman D, Massouras A, Hoffmann AA, Lemaitre B, Deplancke B. 2015. Genetic, molecular and physiological basis of variation in Drosophila gut immunocompetence. *Nat Commun*. **6**:7829.
Brosh O, Fabian DK, Cogni R, Tolosana I, Day JP, Olivieri F, Merckx M, Akilli N, Szkuta P, Jiggins FM. 2022. A novel transposable element-mediated mechanism causes antiviral resistance in Drosophila through truncating the Veneno protein. *Proc Natl Acad Sci U S A*. **119**(29):e2122026119.
Casacuberta E, González J. 2013. The impact of transposable elements in environmental adaptation. *Mol Ecol*. **22**(6):1503–1517.
Catullo RA, Llewelyn J, Phillips BL, Moritz CC. 2019. The potential for rapid evolution under anthropogenic climate change. *Curr Biol*. **29**(19):R996–R1007.
Chuong EB, Elde NC, Feschotte C. 2016. Regulatory evolution of innate immunity through co-option of endogenous retroviruses. *Science* **351**(6277):1083–1087.
Chuong EB, Elde NC, Feschotte C. 2017. Regulatory activities of transposable elements: from conflicts to benefits. *Nat Rev Genet*. **18**(2):71–86.
Dao LTM, Spicuglia S. 2018. Transcriptional regulation by promoters with enhancer function. *Transcription* **9**(5):307–314.
Ding Y, Berrocal A, Morita T, Longden KD, Stern DL. 2016. Natural courtship song variation caused by an intronic retroelement in an ion channel gene. *Nature* **536**(7616):329–332.
Eguchi Y, Bilolikar G, Geiler-Samerotte K. 2019. Why and how to study genetic changes with context-dependent effects. *Curr Opin Genet Dev*. **58–59**:95–102.
Esnault C, Lee M, Ham C, Levin HL. 2019. Transposable element insertions in fission yeast drive adaptation to environmental stress. *Genome Res*. **29**(1):85–95.
Faulkner GJ, Carninci P. 2009. Altruistic functions for selfish DNA. *Cell Cycle* **8**(18):2895–2900.
Frank JA, Singh M, Cullen HB, Kirou RA, Benkaddour-Boumzaouad M, Cortes JL, Garcia Pérez J, Coyne CB, Feschotte C. 2022. Evolution and antiviral activity of a human protein of retroviral origin. *Science* **378**(6618):422–428.
González J, Lenkov K, Lipatov M, Macpherson JM, Petrov DA. 2008. High rate of recent transposable element-induced adaptation in Drosophila melanogaster. *PLoS Biol*. **6**(10):e251.
Green L, Coronado-Zamora M, Radío S, Rech GE, Salces-Ortiz J, González J. 2022. The genomic basis of copper tolerance in Drosophila is shaped by a complex interplay of regulatory and environmental factors. *BMC Biol*. **20**(1):275.
Gröger V, Cynis H. 2018. Human endogenous retroviruses and their putative role in the development of autoimmune disorders such as multiple sclerosis. *Front Microbiol*. **9**:265.
Guio L, Vieira C, González J. 2018. Stress affects the epigenetic marks added by natural transposable element insertions in Drosophila melanogaster. *Sci Rep*. **8**(1):12197.
Hoban S, Kelley JL, Lotterhos KE, Antolin MF, Bradburd G, Lowry DB, Poss ML, Reed LK, Storfer A, Whitlock MC. 2016. Finding the genomic basis of local adaptation: pitfalls, practical solutions, and future directions. *Am Nat*. **188**(4):379–397.
Huang C, Sun H, Xu D, Chen Q, Liang Y, Wang X, Xu G, Tian J, Wang C, Li D, *et al*. 2018. ZmCCT9 enhances maize adaptation to higher latitudes. *Proc Natl Acad Sci U S A*. **115**(2):E334–E341.
Kammenga JE. 2017. The background puzzle: how identical mutations in the same gene lead to different disease symptoms. *FEBS J*. **284**(20):3362–3373.
Koštál V, Korbelová J, Rozsypal J, Zahradníčková H, Cimlová J, Tomčala A, Šimek P. 2011. Long-term cold acclimation extends survival time at 0° C and modifies the metabolomic profiles of the larvae of the fruit fly Drosophila melanogaster. *PLoS One*. **6**(9):e25025.
Larkin A, Marygold SJ, Antonazzo G, Attrill H, Dos Santos G, Garapati PV, Goodman JL, Gramates LS, Millburn G, Strelets VB, *et al*. 2021. Flybase: updates to the Drosophila melanogaster knowledge base. *Nucleic Acids Res*. **49**(D1):D899–D907.
Mackay TFC, Huang W. 2018. Charting the genotype-phenotype map: lessons from the Drosophila melanogaster genetic reference panel. *Wiley Interdiscip Rev Dev Biol*. **7**(1). doi:10.1002/wdev.289.
Mackay TF, Richards S, Stone EA, Barbadilla A, Ayroles JF, Zhu D, Casillas S, Han Y, Magwire MM, Cridland JM, *et al*. 2012. The Drosophila melanogaster genetic reference panel. *Nature* **482**(7384):173–178.
Magwire MM, Bayer F, Webster CL, Cao C, Jiggins FM. 2011. Successive increases in the resistance of Drosophila to viral infection through a transposon insertion followed by a duplication. *PLoS Genet*. **7**(10):e1002337.
Maples T, Rothenfluh A. 2011. A simple way to measure ethanol sensitivity in flies. *J Vis Exp* **19**(48):2541.
Merenciano M, González J. 2023. Two-step CRISPR-Cas9 protocol for transposable element deletion in *D. melanogaster* natural populations. *EcoEvoRxiv*. doi:10.32942/X2P88M.
Merenciano M, Iacometti C, González J. 2019. A unique cluster of *roo* insertions in the promoter region of a stress response gene in *Drosophila Melanogaster*. *Mob DNA*. **10**:10.
Merenciano M, Ullastres A, de Cara MA, Barrón MG, González J. 2016. Multiple independent retroelement insertions in the promoter of a stress response gene have variable molecular and functional effects in Drosophila. *PLoS Genet*. **12**(8):e1006249.
Mi S, Lee X, Li X, Veldman GM, Finnerty H, Racie L, LaVallie E, Tang XY, Edouard P, Howes S, *et al*. 2000. Syncytin is a captive retroviral envelope protein involved in human placental morphogenesis. *Nature* **403**(6771):785–789.
Mihajlovic Z, Tanasic D, Bajgar A, Perez-Gomez R, Steffal P, Krejci A. 2019. Lime is a new protein linking immunity and metabolism in Drosophila. *Dev Biol*. **452**(2):83–94.
Nelson TC, Jones MR, Velotta JP, Dhawanjewar AS, Schweizer RM. 2019. UNVEILing connections between genotype, phenotype, and fitness in natural populations. *Mol Ecol*. **28**(8):1866–1876.
Neyen C, Bretscher AJ, Binggeli O, Lemaitre B. 2014. Methods to study Drosophila immunity. *Methods*. **68**(1):116–128.
Otwinowski J, Nemenman I. 2013. Genotype to phenotype mapping and the fitness landscape of the E. coli lac promoter. *PLoS One* **8**(5):e61570.
Overgaard J, Malmendal A, Sørensen JG, Bundy JG, Loeschcke V, Nielsen NC, Holmstrup M. 2007. Metabolomic profiling of rapid cold hardening and cold shock in Drosophila melanogaster. *J Insect Physiol*. **53**(12):1218–1232.
Pfaffl MW. 2001. A new mathematical model for relative quantification in real-time RT-PCR. *Nucleic Acids Res*. **29**(9):e45.
Port F, Bullock SL. 2016. Augmenting CRISPR applications in Drosophila with tRNA-flanked sgRNAs. *Nat Methods* **13**(10):852–854.
Port F, Strein C, Stricker M, Rauscher B, Heigwer F, Zhou J, Beyersdörffer C, Frei J, Hess A, Kern K, *et al*. 2020. A large-scale resource for tissue-specific CRISPR mutagenesis in. *Elife* **13**(9):e53865.
Rech GE, Bogaerts-Márquez M, Barrón MG, Merenciano M, Villanueva-Cañas JL, Horváth V, Fiston-Lavier AS, Luyten I, Venkataram S, Quesneville S, *et al*. 2019. Stress response, behavior, and development are shaped by transposable element-induced mutations in Drosophila. *PLoS Genet*. **15**(2):e1007900.
Rech GE, Radío S, Guirao-Rico S, Aguilera L, Horvath V, Green L, Lindstadt H, Jamilloux V, Quesneville H, González J. 2022. Population-scale long-read sequencing uncovers transposable elements associated with gene expression variation and adaptive signatures in Drosophila. *Nat Commun*. **13**(1):1948.

Reddy KC, Andersen EC, Kruglyak L, Kim DH. 2009. A polymorphism in npr-1 is a behavioral determinant of pathogen susceptibility in C. elegans. *Science* **323**(5912):382–384.

Rey O, Danchin E, Mirouze M, Loot C, Blanchet S. 2016. Adaptation to global change: a transposable element-epigenetics perspective. *Trends Ecol Evol*. **31**(7):514–526.

Schou MF. 2013. Fast egg collection method greatly improves randomness of egg sampling in Drosophila melanogaster. *Fly (Austin)*. **7**(1):44–46.

Schrader L, Schmitz J. 2019. The impact of transposable elements in adaptive evolution. *Mol Ecol*. **28**(6):1537–1549.

Senft AD, Macfarlan TS. 2021. Transposable elements shape the evolution of mammalian development. *Nat Rev Genet*. **22**(11): 691–711.

Sundaram V, Wysocka J. 2020. Transposable elements as a potent source of diverse cis-regulatory sequences in mammalian genomes. *Philos Trans R Soc Lond B Biol Sci*. **375**(1795): 20190347.

Telonis-Scott M, Hallas R, McKechnie SW, Wee CW, Hoffmann AA. 2009. Selection for cold resistance alters gene transcript levels in Drosophila melanogaster. *J Insect Physiol*. **55**(6):549–555.

Ullastres A, Merenciano M, González J. 2021. Regulatory regions in natural transposable element insertions drive interindividual differences in response to immune challenges in Drosophila. *Genome Biol*. **22**(1):265.

Van't Hof AE, Campagne P, Rigden DJ, Yung CJ, Lingley J, Quail MA, Hall N, Darby AC, Saccheri IJ 2016. The industrial melanism mutation in British peppered moths is a transposable element. *Nature* **534**(7605):102–105.

Villanueva-Cañas JL, Horvath V, Aguilera L, González J. 2019. Diverse families of transposable elements affect the transcriptional regulation of stress-response genes in Drosophila melanogaster. *Nucleic Acids Res*. **47**(13):6842–6857.

Vodovar N, Vinals M, Liehl P, Basset A, Degrouard J, Spellman P, Boccard F, Lemaitre B. 2005. Drosophila host defense after oral infection by an entomopathogenic Pseudomonas species. *Proc Natl Acad Sci U S A*. **102**(32):11414–11419.

Wang X, Huang J, Zhu F. 2018. Human endogenous retroviral envelope protein syncytin-1 and inflammatory abnormalities in neuropsychological diseases. *Front Psychiatry*. **9**:422.

Young AI, Benonisdottir S, Przeworski M, Kong A. 2019. Deconstructing the sources of genotype-phenotype associations in humans. *Science*. **365**(6460):1396–1400.

Zabidi MA, Arnold CD, Schernhuber K, Pagani M, Rath M, Frank O, Stark A. 2015. Enhancer-core-promoter specificity separates developmental and housekeeping gene regulation. *Nature*. **518**(7540):556–559.